# Appendix B

# An Example of the Current State-of-the-Art Geophysical Logging Technology

# Appendix B

# An Example of the Current State-of-the-Art Geophysical Logging Technology

The following is from Schlumberger Inc.

## Introduction

Geophysical logging represents mature, yet constantly evolving, technologies employed as the principal methods of borehole analysis in subsurface characterization.

Wireline logging systems consist of three components (Figure 1):

1) downhole instrument (or sonde) introduced into a borehole that measures one or more physical properties of the formation
2) cable that connects the sonde to the surface, conducting power downhole and transmitting data uphole
3) logging truck that controls sonde location, provides power and houses
4) a computer that controls sonde operation, as well as processes and displays data in real time. The resulting data are shown on a continuous strip chart commonly called a log.

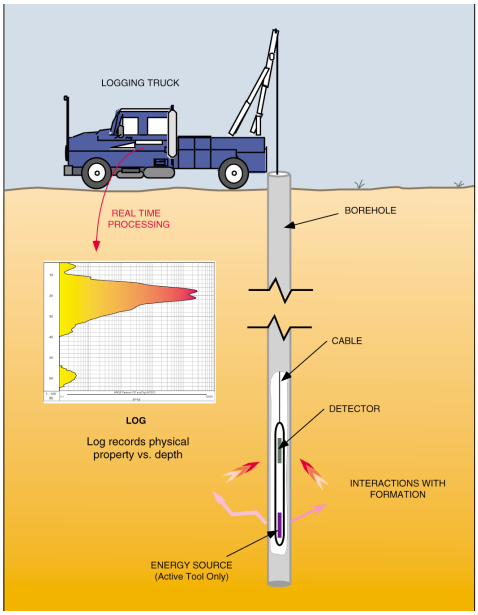


*Figure 1. Logging system*

Geophysical logging systems are designed to give an accurate and precise measurement of formation properties. Formation parameters commonly measured include porosity, moisture content, bulk geochemistry, hydraulic conductivity, orientation of

bedding and fractures, identification and quantification of specific radionuclides and other elements and many others. Logging systems can also be used for downhole sampling and testing.

The integration of multiple logging technologies plus other data types (e.g., geologist's log, core analyses, surface geophysics, hydrologic test analyses) can lead to a fairly comprehensive picture of the shallow subsurface. The precision of the measurements in concert with the potential to measure the same volume repeatedly (i.e., re-enter the same borehole) enhances the use of logging systems for monitoring.

This remainder of this paper presents several recently developed logging technologies that have been applied to aquifer characterization.

## Nuclear Magnetic Resonance Logging

The Combinable Magnetic Resonance* CMR tool uses the nuclear magnetic resonance (NMR) technique to log porous aquifers and predict their producibility (Allen et al., 1997). The unique advantage that NMR provides is a measure of pore size distribution independent of lithology. In the water industry, NMR logging is focused on delineating "producing" from "non-producing" zones and further quantifying formation hydraulic conductivity and total versus effective porosity. In turn, this information can be used to determine optimal well yield.

The CMR tool measures the pore size distribution of the formation from which the porosity, bound and free water distribution, and hydraulic conductivity are estimated. This is achieved by utilizing a large permanent magnet that aligns the non-lattice bound hydrogen along a magnetic field (Figure 2). This process, called polarization, increases exponentially in time with a constant $T_1$. A magnetic pulse from a radio frequency antenna in the CMR tool rotates, or tips, the aligned protons into a plane perpendicular to the polarization. The protons, now aligned in a plane transverse to the polarization field, will start to precess around the direction of the field. The precessing protons sweep out oscillating magnetic fields like a radio antenna. The CMR tool employs a receiver connected to the same antennae used to induce the spin-flipping pulse to measure these magnetic fields. The antennae and receivers are tuned to the resonance frequency of hydrogen nuclei and receive a tiny radio frequency signal from the precessing protons in the formation. Ideally, the spinning protons continue to precess around the direction of the external magnetic field, until they encounter an interaction that would change their spin orientation out of phase with others in the transverse —a transverse relaxation process. The time constant for the transverse relaxation process is called $T_2$. The decay of the precessing signal is the heart of the NMR measurement and is a function of 1) the intrinsic bulk relaxation rate within the borehole fluid, 2) the surface relaxation rate, and 3) diffusion (Kenyon et al 1995).

* Mark of Schlumberger

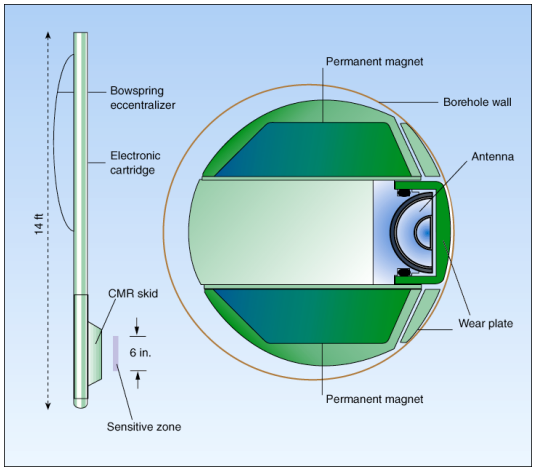


*Figure 2: CMR tool schematic*

In most formations, relaxation times depend on pore sizes. Small pores shorten relaxation times—the shortest times corresponding to clay-bound and capillary-bound water. Large pores allow long relaxation times (Figure 3). Therefore, the distribution of relaxation times is a measure of the distribution of pore sizes (Figure 4).

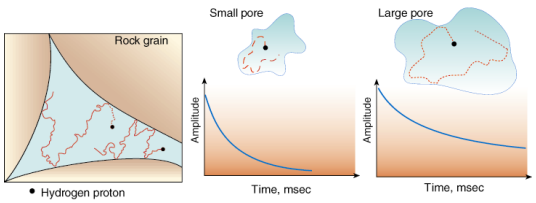


*Figure 3: Relaxation time versus pore size*

$T_2$ relaxation times and their distributions may be interpreted to give other parameters such as hydraulic conductivity, producible porosity and irreducible water saturation. The following equation is commonly used to estimate intrinsic permeability or hydraulic conductivity:

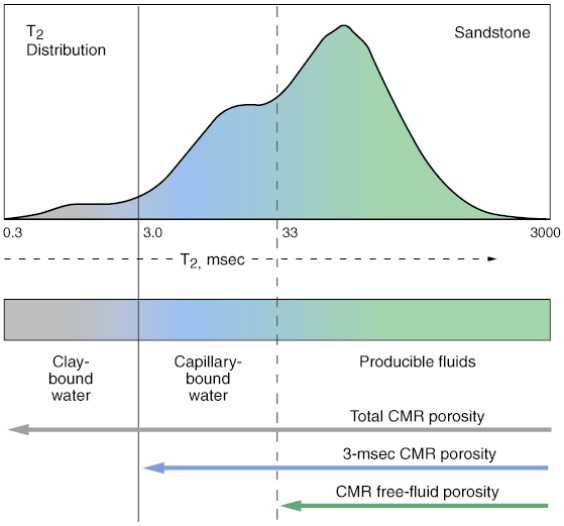


*Figure 4: Pore size as function of relaxation time*

$$k_{NMR} = C(\phi_{NMR})^4 (T_{2,\log})^2$$

$k_{NMR}$ estimated permeability
$\phi_{NMR}$ CMR porosity
$T_{2,\log}$ logarithmic mean of the $T_2$ distribution
$C$ constant, typically 4 for sandstones and 0.1 for carbonates

As this equation indicates, an accurate estimation of hydraulic conductivity requires several core analyses to determine the correct value of $C$.

Figure 5 presents a portion of aquifer logged in New Mexico, US. Each logging track is based on CMR log data and include: effective, capillary, and clay-bound porosity (track1); pore size distribution (track 2); $T_2$ distribution (tracks 3 and 4); hydraulic conductivity in logarithmic units of

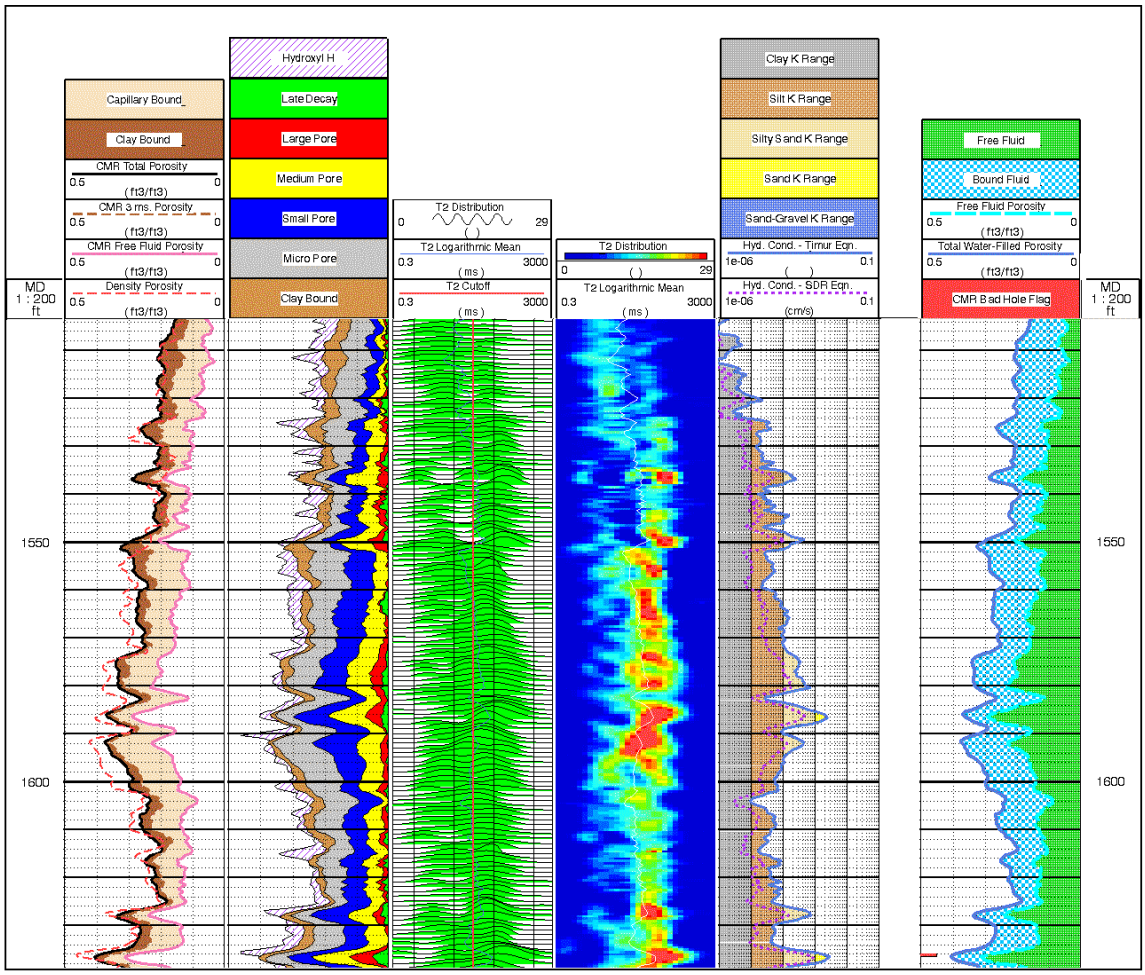


*Figure 5: Nuclear magnetic resonance log of clastic aquifer*

cm/sec (track 5); and total plus effective porosity volumes (track 6). Each horizontal division is equivalent to 2 feet (60 cm) in depth.

All processing is typically performed at the wellsite. This logging tool operates in an open-hole that is either water- or air-filled. Vertical resolution is approximately 20 cm. Valid measurements require a porosity greater than 3%; thus, the measurements are typically insensitive to fractures. For characterization of a fractured aquifer the following tool is recommended.

## Electrical Imager Logging

The Fullbore Formation MicoScanner Imager* FMI tool creates a picture of the borehole wall by mapping its electrical resistivity using an array of 192 small, pad-mounted button electrodes to provide an electrical image of the borehole with a resolution of 5 mm (Ekstrom et al. 1986).

The tool (Figure 6) contains arrays of microresistivity sensors set upon four orthogonal pads and attached flaps. During logging, the lower section of the tool emits current into the formation.

The current is recorded as a series of curves that represent relative changes

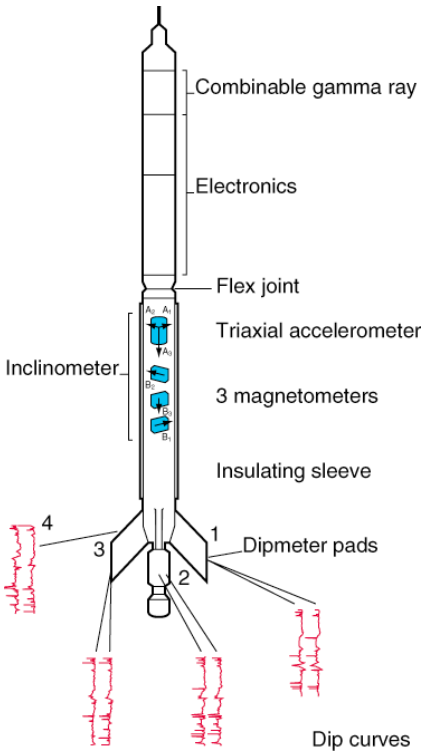


*Figure 6: Schematic of electrical imager tool*

in microresistivity caused by varying electrolytic conduction as a function of pore geometry, fracture geometry, or by cation exchange on the surfaces of clays and other conductive minerals. These effects produce variations on the images in response to porosity, fracture aperture, grain size, mineralogy, cementation and fluid type.

The current intensity measurements recorded in each button electrode, which reflect the microresistivity variations, are converted to variable-intensity color images. The lightest tone representing the most resistive samples, and the darkest the most electrically conductive (Figure 7). The color is synthetic and does not indicate lithology or the true color of the formation.

A planar surface cutting the borehole describes an ellipse on the cylindrical borehole boundary surface. If the

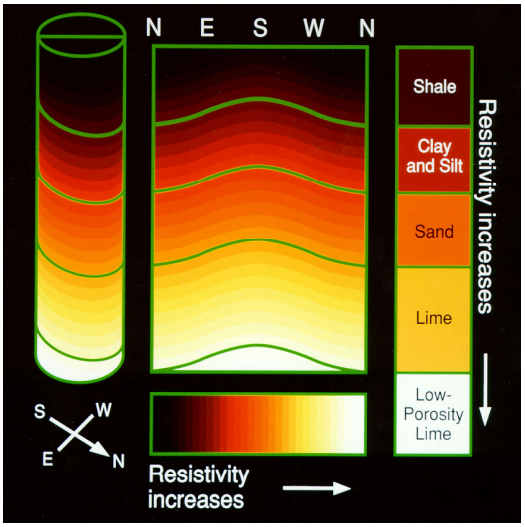


*Figure 7: Image generation*

cylinder representing the borehole side is cut open and unrolled to become a flat surface, the ellipse becomes a sine wave. The amplitude of this sinusoid is proportional to the apparent dip of the intersecting plane, and the orientation of the trough indicates its apparent azimuth.

A triaxial accelerometer permits determination of tool position, and three magnetometers allow determination of tool orientation. With these inputs, the orientation of all planar features that intersect the borehole wall (e.g., bedding and fractures) is calculated. Dip is represented on a log by a small circle with a tail. The position of the circle along the horizontal axis portrays dip magnitude, ranging from 0 to 90° on the right. Tail direction is analogous to dip direction, with north at the top of the log.

Fractures form a fairly unambiguous feature on this type of log. Dark (electrically conductive) lines that typically cut across bedding, and sometimes parallel it, are usually considered open, water-filled fractures. Healed fractures typically appear light instead of dark. The image does not tell

whether a fracture contributes to aquifer production; it tells only that the fracture

is present at the wellbore (Bourke et al. 1989). Determining whether the fracture will produce water, or act as a hydraulic conductivity path or barrier requires the calculation of fracture aperture.

Once fractures are mapped and their orientation is calculated, then fracture density and spacing can be computed. Fracture aperture can be estimated through additional data processing.

Forward modeling of the electrical field present around a fracture using a finite-element code was used to determine the relationship between fracture aperture, formation resistivity, mud resistivity, and additional current flow caused by the presence of the fracture (Luthi and Souhaité 1990). The resulting equation is:

$$A = \frac{W}{R_m \bullet c}\left(\frac{R_{xo}}{R_m}\right)^{1-b}$$

$W$ fracture width (mm)

$R_{xo}$ formation resistivity

$R_m$ water resistivity

$A$ integrated excess current caused by presence of fracture

$c$ coefficient obtained numerically from forward modeling

$b$ exponent obtained numerically from forward modeling

Note that formation resistivity can not be determined with the imaging tool; it requires the integration of a conventional resistivity or induction log data.

A three-step process to detect, trace, and quantify fractures is used. The fractures are typically mapped as part of the interpretation process; the trace for each fracture is determined by mapping where electrical conductivity significantly exceeds local matrix conductivity followed by line sharpening; and apertures are computed for all fracture locations. This method allows the detection of fractures of 10 μm aperture and may resolve fractures about 1 cm apart.

Figure 8 presents a portion of a log collected in a fractured basalt aquifer. This log depicts primarily the FMI results that include: images (tracks 3 and 5), calculated apertures in logarithmic scale (track 4), fracture orientation (track 6), fracture trace length and density (track 7). Each fracture trace with aperture is superimposed on the image in track 3.Track 2 depicts different porosity logs, and it includes the fracture porosity. Each horizontal division is equivalent to 2 feet (60 cm) in depth.

Fully processed images and dip data can also be provided at the wellsite in real time. Fracture analysis requires further processing. The tool is designed to work in a water-filled, open borehole. Unlike optical televiewers, this tool is unaffected by water opacity.

## References

Allen, D., S. Crary, B. Freedman, M. Andreani, W. Klopf, R. Badry, C. Flaum, B. Kenyon, R. Kleinberg, P. Gossenberg, J. Horkowitz, D. Logan, J. Singer, and J. White. 1997. “How to Use Borehole Nuclear Magnetic Resonance.” Oilfield Review, v. 9, n. 2, p. 34 – 57.

Bourke, L., P. Delfiner, J. Touiller, T. Fett, M. Grace, S. Luthi, O. Serra and E. Standen. 1989. “Using Formation MicroScanner Images.” The Technical Review, v. 37, n. 1, p. 16 – 40.

Ekstrom, M.P., C.A. Dahan, M.Y. Chen, P.M. Lloyd, and D.J. Rossi. 1986. “Formation Imaging with Microelectrical Scanning Arrays.” Transaction of the SPWLA 27th Annual Logging Symposium, Houston, paper BB.

Kenyon, B., R. Kleinberg, C. Straley, G. Gubelin, and C. Morris: 1995. “Nuclear Magnetic Resonance Imaging—Technology for the 21st Century.” Oilfield Review, v. 7, n. 3, p. 19 – 33.

Luthi, S.M. and P. Souhaité. 1990. “Fracture Apertures from Electrical Borehole Scans.” Geophysics, v. 55, n.7, p. 821 – 833.

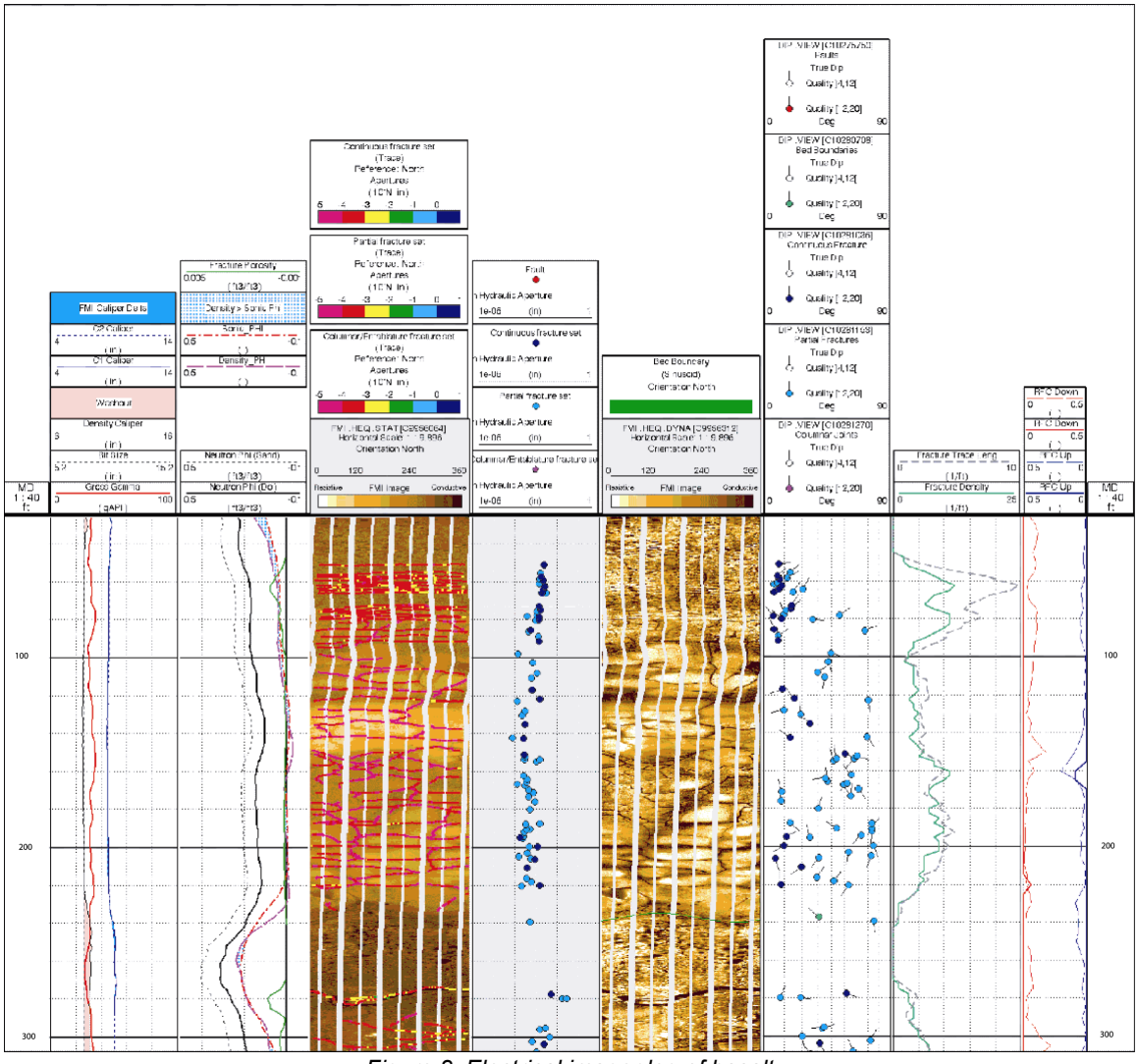

*Figure 8: Electrical imager log of basalt*